micro

MDPI

Article

Graphene Formation through Spontaneous Exfoliation of Graphite by Chlorosulfonic Acid: A DFT Study

Alfredo Bol-Arreba [1,2,*], Isabel G. Ayala [1] and Nicolás A. Cordero [1,2,3]

[1] Physics Department, Universidad de Burgos, E-09001 Burgos, Spain
[2] International Research Center in Critical Raw Materials for Advanced Industrial Technologies (ICCRAM), Universidad de Burgos, E-09001 Burgos, Spain
[3] Institute Carlos I for Theoretical and Computational Physics (IC1), E-18016 Granada, Spain
* Correspondence: alf_bol@ubu.es

Abstract: Using exfoliating agents is one of the most promising ways for large-scale production of liquid dispersed graphenic materials from graphite. Therefore, it is crucial to know the reason why some molecules have a larger exfoliating power than others. The highest reported experimental yield for the liquid phase single-surfactant spontaneous exfoliation of graphite, i.e., without sonication, has been obtained using chlorosulfonic acid. The ability of this acid to disperse graphite is studied within the framework of Density Functional Theory (DFT). Equilibrium configurations, electron transfers, binding energies, and densities of states are presented for two acid concentrations and for two situations: adsorption (on monolayer and bilayer graphene) and intercalation (in between simple hexagonal and Bernal-stacked bilayer graphene). Experimental exfoliation power and dispersion stability are explained in terms of charge transfer—the largest found among several studied exfoliating and surfactant agents—facilitated by the good geometrical matching of chlorosulfonic acid molecules to constituent carbon rings of graphene. This matching is in the origin of the tendency toward adsorption of chlorosulfonic acid molecules on graphene monolayers when they separate, originating the charging of the monolayers that precludes their reaggregation.

Keywords: graphene; exfoliation; chlorosulfonic acid; DFT

Citation: Bol-Arreba, A.; Ayala, I.G.; Cordero, N.A. Graphene Formation through Spontaneous Exfoliation of Graphite by Chlorosulfonic Acid: A DFT Study. *Micro* **2023**, *3*, 143–155. https://doi.org/10.3390/micro3010011

Academic Editor: Hiroshi Furuta

Received: 27 November 2022
Revised: 23 January 2023
Accepted: 24 January 2023
Published: 31 January 2023

1. Introduction

The extraordinary properties of graphene have given rise to the proposal of numerous applications in different fields. However, its commercial use requires high-yield production methods that guarantee stable, standardized production conditions. Graphene production uses procedures with low yields that have not fully reached these requirements.

Graphene production methods are conventionally classified into two different approaches: top-down methods, which produce graphene from a 3D macroscopic source, i.e., graphite, and bottom-up methods, those in which graphene is obtained by assembling molecular building blocks.

The technique used for the first time to produce graphene, micromechanical cleavage [1], is an example of the first approach. However, this mechanical method has yields just suitable for fundamental research and prototype devices. Another production method, also belonging to the top-down approach, is liquid phase exfoliation: graphene is produced by exfoliation of graphite with or without ultrasonication of the samples in a solvent that also prevents reaggregation. This method can be scaled up for a larger production and has been proposed as a route to industrial processing [2]. There are several solvents with different yields, such as dimethylformamide [3], proposed for rather illustrative purposes, or N-methyl-pyrrolidone, with yields from 0.01 mg mL^{-1} to 1.2 mg mL^{-1}, depending on the sonication rate [4,5]; tetrahydrofuran has also been used, with a 0.16 mg mL^{-1} [6] yield, as well as cyrene with a 0.24 mg mL^{-1} [7] yield. Exfoliation has been tried in aqueous solution

with the aid of several surfactants: sodium dodecylsulfate (SDS) [8], sodium dodecyl benzenesulfonate (SDBS) [9] (0.002–0.05 mg mL^{-1} yield), sodium cholate [8,10] (0.3 mg mL^{-1} yield), amphiphilic peptides [11], cetyltrimethylammonium bromide (CTAB) [8], perylene-based bolaamphiphilic detergents [12], nonylphenolethoxylate (NPE) [8], anionic aromatic surfactants [13], sodium N-lauroylsarcosinate hydrate (SNLS) [14], *sapindus mukorossi* [15] (>1 mg mL^{-1} yield), or amine-based solvents [16] with yields as high as 15 mg mL^{-1} when few-layer graphene powder is used as a precursor. In some cases, mixtures of two or more surfactants have been used [17–20]. Ionic liquids, salts with a melting point below 100 °C, are another family of compounds with promising exfoliation candidates that are also suitable for the stabilization of the resulting solutions [21,22]. For example, dispersions with a concentration of 0.95 mg mL^{-1} are obtained with 1-butyl-3-methylimidazolium bis(trifluoromethylsulfonyl)imide, after sonication, 0.081 mg mL^{-1} with 1-benzyl-3-methylimidazolium ([(Bn)mim] [NTf_2]), and 5.8 mg mL^{-1} with bis (trifluoromethanesulfonyl)imide ([$(Bn)_2$im][NTf_2]) [23].

There are other strategies, such as the dispersion of graphene oxide [24,25], that require an eventual reduction or starting the exfoliation from turbostratic graphite [26]. This kind of graphite has its constituent graphenic sheets slightly rotated around the axis perpendicular to the layers with respect to the conventional AB stacking, and as a consequence, its interlayer separation distance grows to 3.45 Å from the 3.35 Å of the tightly bound AB-stacked highly oriented pyrolytic graphite (HOPG). This tiny transversal expansion represents, according to Tour and coworkers, an advantage that increases the yield when liquid dispersions are generated.

To the best of our knowledge, the highest reported yield until 2021 for the liquid phase spontaneous exfoliation method using a single exfoliating agent (arround 2 mg $mL^{-1)}$), i.e., exfoliation of graphite without sonication, was obtained by Behabtu and coworkers using chlorosulfonic acid [27]. This year, Kretinin et al. [28], using the same acid and adding pyrene, more than doubled the yield, reaching an outstanding ∼5 wt%. Chlorosulfonic acid (CSA, also known as sulfurochloridic acid) has also been used to exfoliate and expand graphite oxide for the bulk production of graphenic materials [29] and to exfoliate inorganic 2D transition metal dichalcogenides [28,30] or boron nitride [28]. The advantage of avoiding the sonication process is the production of so-called pristine graphene, i.e., graphene with the same defects present in the graphite precursor and with no oxidized areas [31]. One of the negative sides of the use of CSA is its poor dispersion stability; trace amounts of moisture are sufficient to cause reaggregation and restacking [28].

A conclusion that can be reached from these previous works is that the obtention of liquid dispersed graphene solutions requires a starting step, i.e., the trigger of the exfoliation process, which consists of an initial sheet separation, either with a Coulomb mechanism or boosted by the action of CSA [27,28] or steric, because of the removal of the perfect AB stacking [26]. Our study of the interaction between graphene and CSA attempts to determine why CSA is especially efficient for this. In order to understand the ability of HSO_3Cl to exfoliate graphitic samples, we have studied the effect on the geometrical and electronic properties (equilibrium geometries, binding energies, charge transfers, and densities of states) of monolayer graphene (MLG) and bilayer graphene (BLG) when acid molecules are adsorbed on the first and second system and are intercalated between the constituent layers of the second. We have chosen Bernal [32] AB stacking as well as simple hexagonal AA stacking, as in other previous works [33–35], because the latter is a common crystallographic structure in graphite intercalation compounds [36,37]. According to our calculations, simple hexagonal stacking is the preferred structure for chlorosulfonic-acid-intercalated BLGs, but AB stacking is more stable for clean bilayers. AA stacking is also found in epitaxially grown graphite [38], in carbon nanofilms grown from graphite oxide [39], and in some finite BLGs [40]. However, the stacking selected to obtain magnitudes and properties is not crucial, since all BLGs have nearly the same binding energy [41–43] and electron band structure [44] when the separation between the layers is greater than 4 Å.

2. Materials and Methods

The calculations of the interaction of chlorosulfonic acid with graphene layers have been performed using DFT [45] at the LDA [46] level as implemented in Dacapo [47]. LDA has been chosen because interactions among graphitic structures are suitably described [48], and it performs better than gradient-corrected approximations (GGAs) of hybrid functionals for these systems [49–52].

Dacapo is a code that uses supercells and a plane wave basis set for valence electrons, valence–core interactions being described through Vanderbilt ultrasoft pseudopotentials [53]. The pseudopotential used to describe sulfur atoms contains non-linear core–valence interaction corrections. The plane wave cutoff has been set to 350 eV and the density cutoff to 500 eV. Total energies were converged to 10^{-5} eV, and all atomic positions were relaxed until Cartesian forces on each atom were below 0.05 eV/Å. Similar techniques have been previously used for studying the interaction of sulfuric acid and Li atoms with graphene [33,54], of surfactant molecules with a sulfuric group with a (5,5) carbon nanotube [55], sulfuric acid on bilayer graphene [34], and the catalytic activity of palladium on a graphene surface [56].

In order to simulate two different acid concentrations, we have used two different hexagonal graphene supercells. They are shown in Figure 1. One of the supercells contains 18 C atoms per layer, and putting a HSO_3Cl molecule in it gives a high concentration of one acid molecule per 36 carbon atoms in the bilayer supercell. A lower concentration is simulated by placing a HSO_3Cl molecule in a supercell that has 32 atoms per graphene layer. The height of the supercells has been set to 30 Å to avoid interactions between adjacent supercells along the z axis and simulate a completely exfoliated equilibrium state.

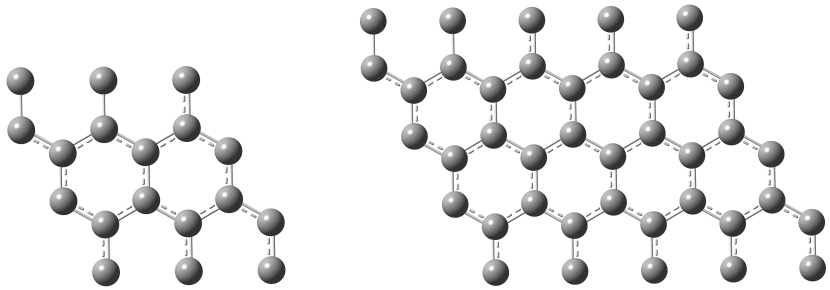

Figure 1. Graphene unit cells used for different acid concentrations (**left**, high; **right**, low). High/low concentration corresponds to one acid molecule in a supercell with 18/32 C atoms for MLG and 36/64 atoms for BLG.

The k-points in reciprocal space were selected using the Monkhorst–Pack scheme [57]. The number of points for geometry optimizations as well as for energy and charge transfer calculations was $2 \times 2 \times 1$ for low concentration and $4 \times 4 \times 1$ for high concentration. For density of states (DOS) calculations, these numbers were increased to $18 \times 18 \times 1$ and $24 \times 24 \times 1$, respectively.

3. Results and Discussion

In order to understand the ability of chlorosulfonic acid to exfoliate graphite, we have studied the adsorption of the acid molecule on MLG and on BLG as well as the intercalation between the two layers of BLG. We compare the results with those previously obtained for sulfuric acid [34] and sodium bisulfate [35]. We also propose an explanation about the reaggregation inhibitor role of chlorosulfonic acid, and finally, we present results on the electronic properties of graphene flakes upon chlorosulfonic acid adsorption.

3.1. The HSO_3Cl Molecule and Its Geometrical Matching with Carbon Rings

As there are no experimental data available for the molecular structure of the chlorosulfonic acid molecule, we show in Table 1 bond lengths and planar and dihedral angles calculated according to the scheme described in the previous section. A comparison with

calculations performed with Gaussian 09 [58], with a 6-31G** basis set and the LDA exchange correlation functional is presented. As a reference, second-order Møller–Plesset calculations were also performed with Gaussian 09. The results correspond to the structure shown in Figure 2. It is tetrahedral, with the sulfur atom occupying an endohedral position and the three oxygen atoms and the chlorine atom at the vertices of the tetrahedron. The hydrogen atom is off the plane defined by the sulfur, chlorine, and oxygen atom 1, to which it is bonded. Similar geometrical results have been obtained by Yokoyama et al. [56] for SO_4 adsorbed on graphene. It should be noted that the distance between this oxygen atom and the chlorine atom is 2.82 Å, whereas the maximum diagonal in each hexagonal carbon ring in graphene is 2.84 Å. The mean value of the S-O distance is 1.5 Å, a rather similar value to the C–C bond length, 1.41 Å. The good geometrical matching of the chlorosulfonic acid molecule with the carbon atom rings of graphene is shown in the lower panel of Figure 3, where the acid molecules adsorbed on graphene are depicted for the most stable configuration. The hydrogen atom, the sulfur atom, and the chlorine atom are almost confronted with the carbon atoms of the constituent rings.

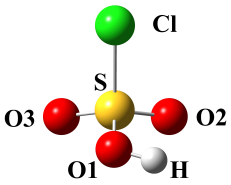

Figure 2. Geometric structure of a HSO_3Cl molecule.

Table 1. Calculated bond lengths (in Å), planar and dihedral angles (in degrees) for the chlorosulfonic acid molecule. Gaussian/Dacapo compared data.

Distances				**Planar Angles**				**Dihedral Angles**			
	Gaussian		**Dacapo**		**Gaussian**		**Dacapo**		**Gaussian**		**Dacapo**
	LDA	**MP2**	**LDA**		**LDA**	**MP2**	**LDA**		**LDA**	**MP2**	**LDA**
S-O1	1.61	1.62	1.60	O1-S-Cl	100.4	100.3	100.3	O1-S-Cl-O2	111.1	111.0	110.7
S-O2	1.44	1.45	1.43	O2-S-Cl	106.9	107.0	106.6	O2-S-Cl-O3	135.6	135.9	135.7
S-O3	1.45	1.41	1.41	O3-S-Cl	107.5	107.5	107.4	O3-S-Cl-O1	113.3	113.1	113.6
S-Cl	2.05	2.05	2.07	S-O1-H	107.4	107.5	108.7				
O3-H	0.98	0.97	0.98								

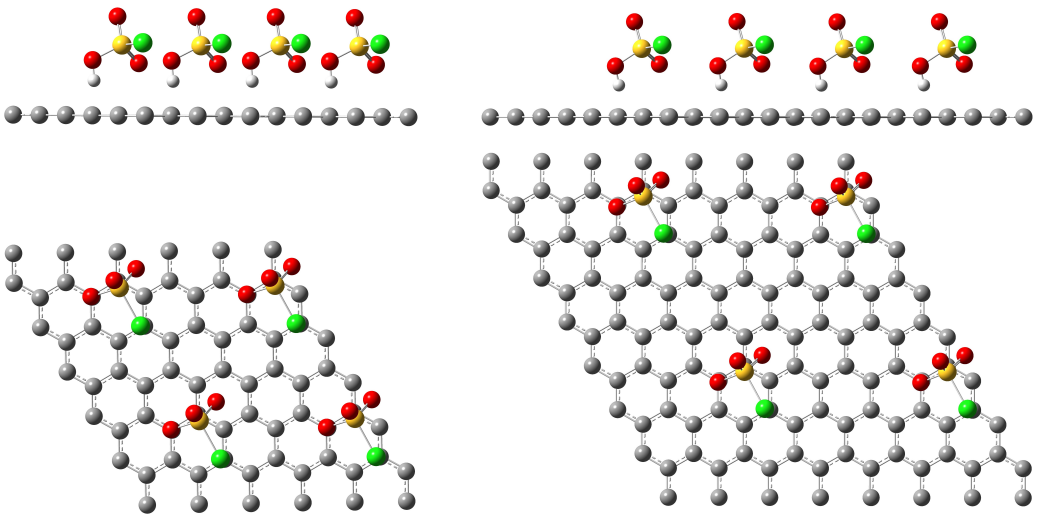

Figure 3. Side (**upper row**) and front (**lower row**) views of 2 × 2 unit cells of chlorosulfonic acid adsorbed on graphene for two concentrations: high (**left panels**) and low (**right panels**).

3.2. Interaction Energies and Charge Transfer to MLG

The adsorption energy is defined as the difference between the energy of the adsorbed configuration and the sum of the energies of the isolated acid molecule and the clean MLG:

$$E_{\text{ads}} = E(\text{MLG}) + E(\text{HSO}_3\text{Cl}) - E(\text{MLG} + \text{HSO}_3\text{Cl ads}).$$

A similar definition can be stated for BLG. This definition corresponds to the adsorption energy per acid molecule and takes advantage of the presence of a single acid molecule in the unit cell. Results are shown in Table 2. Those of sulfuric acid [33] and sodium bisulfate [35] are also shown for the sake of comparison.

Table 2. Calculated adsorption energies (E_{ads}) as well as electron transfers (ΔQ_{ads}) to each acid molecule for chlorosulfonic acid for two concentrations: low (one molecule per 32 carbon atoms in MLG) and high (one molecule per 18 carbon atoms in MLG). Values corresponding to sulfuric acid and sodium bisulfate are given for comparison.

		Chlorosulfonic Acid		**Sulfuric Acid [33]**		**Sodium Bisulfate [35]**	
	Conc.	E_{ads} **(eV)**	ΔQ_{ads} **(*e*)**	E_{ads} **(eV)**	ΔQ_{ads} **(*e*)**	E_{ads} **(eV)**	ΔQ_{ads} **(*e*)**
MLG	Low	0.36	0.44	0.29	0.30	0.44	0.11
	High	0.34	0.36	0.34	0.26	0.54	0.04
AB-BLG	Low	0.35	0.43				
	High	0.33	0.36				
AA-BLG	Low	0.42	0.43				
	High	0.49	0.36				

As expected, the adsorption of chlorosulfonic acid is an exothermic process. This energy, in the case of MLG, is bigger than the corresponding adsorption energy of sulfuric acid but smaller than that of sodium bisulfate, which belongs to the family of molecules with a sulfonated head group with a Na atom, known to have poorer surfactant effects than the acids [59–61]. However, there is a significant difference with respect to the charge transfer, calculated using Mulliken population analysis [62], as shown in Table 2; it is much higher for chlorosulfonic acid than for sulfuric acid or sodium bisulfate, for both concentrations analyzed. In fact, charge transfer in the case of chlorosulfonic acid is 46% larger than in the case of sulfuric acid, and four-fold larger than in the case of sodium bisulfate. Irrespective of the considered exfoliating agent, when concentration increases, charge transfer diminishes, but the general trend is maintained, i.e., with chlorosulfonic acid being the species with higher charge transfer, particularly in comparison with sodium bisulfate. This fact is in accordance with the relative insensitivity with respect to concentration of the surfactant effect of molecules with a sulfonated head group with a Na atom and the clear relation between concentration and exfoliating power in the case of chlorosulfonic acid [27]. This large charge transfer could be at the root of the Coulombic repulsion between charged flakes, and it can also help to understand the huge amount of exfoliated but not intercalated graphene flakes in chlorosulfonic acid graphene dispersed solutions, according to Kretinin's results [28] (see below for more details).

3.3. Interaction Energies and Charge Transfer to BLG

In the next step, we have studied the adsorption of chlorosulfonic acid on one of the constituent layers of BLG and the intercalation between two graphene layers. Their equilibrium interlayer distance (d_{eq}) and interlayer interaction energies (E_{int}), i.e., exfoliation energy, have been calculated for AB Bernal stacking and for AA stacking, and they are shown in Table 3 and compared with the experiment and other calculations. Another comparison can be done with the interlayer separation of turbostratic graphene, which is easier to exfoliate according to Tour's group experiments, that is 0.1 Å larger that the 3.35 Å of the AA-stacked case [26]. Interlayer distances are accurately reproduced, but it is not the same for exfoliation energy, which is known to be poorly predicted by LDA

calculations [41]. Nevertheless, this fact does not affect our study, since it is not based on absolute energies but on relative energy differences among different surfactants, all of them calculated with the same computational method.

The ranking of the adsorption energy of the acid molecule to MLG and BLG in Tables 2 and 3 shows that the strongest interaction of the molecule happens with AA-BLG; the weakest is with AB-BLG, being the interaction with MLG intermediate. The key to understanding this behavior is the interaction between layers for both stackings, which is stronger in the AB case; AB-BLG is more stable and has a larger binding energy (by 5.6 meV/atom) and a smaller interlayer separation (by 0.3 Å, see Table 3) than AA-BLG. This result is easy to explain in terms of electronic density overlapping: electron-rich areas of the constituent monolayers are confronted in the case of AA stacking, while they match the poorer ones in the AB stacking case. A point that reinforces this idea is the value of charge transfer from graphene layers, which is basically the same for the three situations considered.

Table 3. Equilibrium interlayer distances (d_{eq}) and interlayer interaction energies (E_{int}) for AB-BLG and AA-BLG.

	AA Stacking		**AB Stacking**	
	d_{eq} **(Å)**	E_{int} **(meV/at)**	d_{eq} **(Å)**	E_{int} **(meV/at)**
Exp.	3.55	-	3.34 [63]	60.5 [64]
This work	3.65	7.0	3.35	12.6
Ref. [65]	3.66	9.8	3.30	19.6
Ref. [66]	3.59	-	-	-
Ref. [41]	3.57	-	3.34	48.0

Four unit cells of the intercalated high- and low-acid-concentration samples are shown in Figure 4. As in the case of adsorption on MLG, at the equilibrium configuration, the hydrogen atom, the chlorine atom, and one of the oxygen atoms are faced with three carbon atoms of one of the graphene layers. Moreover, in the intercalated AA-BLG case, the third oxygen atom is confronted with a carbon atom of the second graphene layer. This detail cannot be appreciated in Figure 4 but can be inferred from Figure 3. Notice that the chlorosulfonic acid matching with both layers is a consequence of the AA stacking, but this geometrical matching will also occur in the case of AB stacking by performing a rotation of the acid molecule in the interlayer by 30° around the axis defined by the O–H bond.

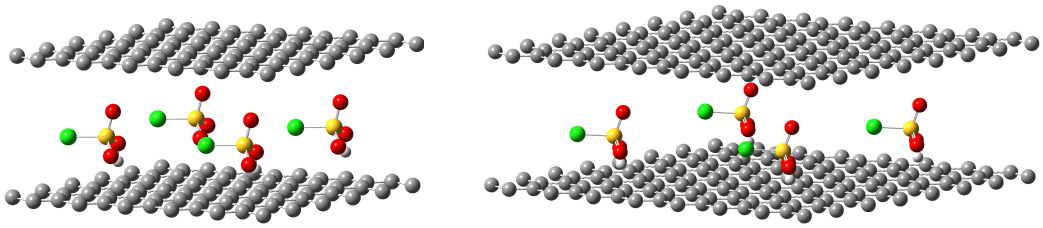

Figure 4. Chlorosulfonic acid in between AA-BLG (2 × 2 × 1 supercells) for two concentrations.

Intercalation energy per acid molecule is defined as

$$E_{int} = E(\text{BLG}) + E(\text{HSO}_3\text{Cl}) - E(\text{BLG} + \text{HSO}_3\text{Cl int}).$$

At sufficiently high acid concentration, intercalation is also an exothermic process. According to the data shown in Table 4 (where, for the sake of comparison, the data for sulfuric acid [34] and sodium bisulfate [35] are also shown), at high acid concentration, intercalation is an energetically favorable process, and in fact, intercalation energy for chlorosulfonic acid at the highest concentration is the largest for the three considered species, in accordance with the spontaneous nature of graphene exfoliation in sufficiently

concentrated chlorosulfonic acid [27,28], i.e., without the addition of energy through sonication. Calculated results are in reasonable agreement with the experimental results by Kretinin [28]. The statistical distribution of the interlayer distance of spontaneously exfoliated flakes of graphene is reported (see Figure 2g in this reference) to range from 2 to 10 Å, with a maximum concentration of samples at around 3–4 Å (possibly corresponding to non-exfoliated ones), followed by a great amount of samples in the range 4–7 Å (possibly corresponding to exfoliated but not yet intercalated samples) and, finally, with a large amount of representatives in the range 7–8 Å. This distance is in fair agreement with exfoliated and intercalated samples with chlorosulfonic acid or, as in this experiment, its sulfonate derivative.

Table 4. Calculated equilibrium interlayer distance (d_{eq}), intercalation (E_{int}) energy into BLG, adsorption energy (E_{ads}) on BLG, electron transfer from the graphene bilayer to each acid molecule (ΔQ_{int}) for chlorosulfonic and sulfuric [34] acids, for sodium bisulfate [35], and two concentrations: low (one molecule per 64 carbon atoms) and high (one molecule per 36 carbon atoms).

		Chlorosulfonic Acid				**Sulfuric Acid [34]**			**Sodium Bisulfate [35]**		
Conc.	**Stacking**	d_{eq} **(Å)**	E_{int} **(eV)**	E_{ads} **(eV)**	ΔQ_{int} **(*e*)**	d_{eq} **(Å)**	E_{int} **(eV)**	ΔQ_{int} **(*e*)**	d_{eq} **(Å)**	E_{int} **(eV)**	ΔQ_{int} **(*e*)**
Low	AB	7.78	−0.25	0.43	0.41						
	AA	7.87	0.08	0.42	0.54	7.6	0.09	0.48	7.8	0.22	0.14
High	AB	7.85	0.01	0.49	0.39						
	AA	8.00	0.34	0.42	0.42	7.6	0.24	0.39	7.8	0.33	0.09

Another point to be considered is the difference in the intercalation energy for both stackings. Data in Table 4 reveal that intercalation is a more exothermic process when it occurs in AA-stacked systems, possibly because the interlayer distance for clean AA-BLG is 0.3 Å larger than for AB-BLG. The distance between graphene layers with an intercalated acid molecule in between, as shown in Table 4, is 0.3–0.4 Å higher in the case of chlorosulfonic acid than in the case of sulfuric acid, due to the size of the Cl atom. The comparison with respect to sodium bisulfate is also favorable to chlorosulfonic acid, but the effect is not so pronounced (0.1–0.2 Å higher in the case of chlorosulfonic acid).

Interlayer distance increases slightly when chlorosulfonic acid concentration increases, but this behavior is not observed in the case of sulfuric acid or sodium bisulfate. This effect cannot be explained in steric terms but rather in charge transfer terms. According to the data shown in Table 4, charge transfer from the chlorosulfonic acid molecule is the largest of the three considered species. This computational result has also been experimentally found by Cao et al. [11], who have determined that charge is an important parameter in predicting the graphite exfoliating efficiency of several molecules, being that the anionic ones are the more favorable compared to the cationic ones. Charge transfer from graphitic walls to chlorine (and other halogen atoms) has been recently predicted for the encapsulation of these atoms inside single-walled carbon nanotubes [67].

3.4. The Efficiency of Chlorosulfonic Acid to Prevent Reaggregation

Exfoliation efficiency cannot be explained just in terms of layers' separation ability, but the preclusion of reaggregation must also be taken into account. To gain insight into this point, we have studied the behavior of the chlorosulfonic acid molecule with slightly modified interlayer separations with respect to the equilibrium configuration. The results are shown in Table 5, where intercalation energies, distances of the chlorosulfonic acid to both MLG in AA-BLG, and charge transfers are shown for several interlayer separations for the low-concentration case. References in the chlorosulfonic acid molecule for the determination of these distances are the hydrogen atom and oxygen atom number 3, according to Figure 2, and, in the MLG constituting the AA-BLG, the nearest neighboring carbon atoms.

Table 5. Intercalation energy (E_{int}) into BLG, distances from chlorosulfonic acid molecule to constituent MLG taking as a reference the H atom, d(H–C), and the O3 atom, d(O–C) (see Figure 2), and electron transfers from BLG to each acid molecule (ΔQ_{int}) for several interlayer distances (d_{intl}) around equilibrium configuration. (Calculations for the low concentration regime).

d_{intl} (Å)	E_{int} (eV)	d(H–C) (Å)	d(O–C) (Å)	ΔQ_{int} (e)
7.55	0.04	1.86	2.71	0.56
7.71	0.06	1.88	2.81	0.55
7.87	0.08	1.90	2.93	0.54
8.20	0.07	1.93	3.20	0.53
8.56	0.04	1.96	3.49	0.51

As can be inferred from Table 5, while the separation between both MLGs increases 1.01 Å from 7.55 Å to 8.56 Å the distance of the hydrogen atom to its nearest neighboring carbon atom varies by 0.09 Å, and the distance of the oxygen atom to its nearest neighboring carbon atom varies by 0.78 Å, i.e., chlorosulfonic acid molecules remain adsorbed to one of the layers, with 0.54 electrons transferred from the BLG to the acid molecule. It should be noted that the distribution of the negative charge gained by this molecule is rather symmetrical, i.e., it comes from both component layers (0.29 and 0.25 electrons, respectively), even though they are well separated (for the maximum intercalation energy, 7.87 Å, a separation that doubles the equilibrium distance) and one of them has the acid molecule much closer than the other.

The ability of chlorosulfonic acid to charge both layers and, consequently, to provide a Coulombic mechanism to preclude reaggregation could be an explanation for the stability of graphene dispersions in this acid. This fact is in accordance with the results of Kretinin [28] for the spontaneous exfoliation with chlorosulfonic acid and those of Englert et al. [12], who reported an efficient graphene production method based on bolaamphiphilic detergents.

3.5. Electronic Properties

The effect on the electronic properties of mono- and bilayer graphene as a consequence of the adsorption and intercalation of chlorosulfonic acid has been studied by means of the DOS of these systems with and without chlorosulfonic acid. In Figure 5, the DOS of a clean MLG is compared with the DOS of the MLG with an adsorbed chlorosulfonic acid molecule for the two unit cells used in this work. In spite of the electron transfer from MLG to the acid, the basic features of the DOS remain unaltered. The role of the acid molecules amounts to the superposition of molecular states to the DOS of the MLG. In particular, near the neighborhood of the Fermi level, there is no modification of the DOS; as a consequence, the zero-gap semiconductor nature of graphene does not depend on whether chlorosulfonic acid is adsorbed or not, irrespective of the acid concentration.

It is known [42,68–70] that the DOS of BLG is very similar to that of MLG, and in fact, both appear almost completely superimposed in Figure 6. The most significant difference is near the Fermi level; while the DOS of MLG vanishes for this energy, this does not happen for BLG (with an equilibrium interlayer distance of 3.6 Å), as can be seen in the inset of the figure, in agreement with earlier works [68]. Note that the DOS of MLG is very small but not exactly zero at the Fermi energy level, because of the plotting technique of smearing the eigenvalues with finite-width Gaussians.

The inset of Figure 6 shows that the DOS of BLG (with an interlayer distance of 3.6 Å) is very similar to the DOS of BLG with an intercalated acid molecule, notwithstanding the large separation between graphene layers (7.9 Å and 8.0 Å for low and high concentrations, respectively). This fact can be interpreted as a manifestation of incomplete decoupling, probably because of the large electron transfer from the layers to the acid molecule. This partial decoupling is a characteristic of this acid and different to the behavior observed in experiments with K intercalated graphite [71], though in that case, the potassium atom acts as an electron donor, and here the chlorosulfonic acid is an acceptor. This behavior is also different to that predicted for other intercalants [34,35].

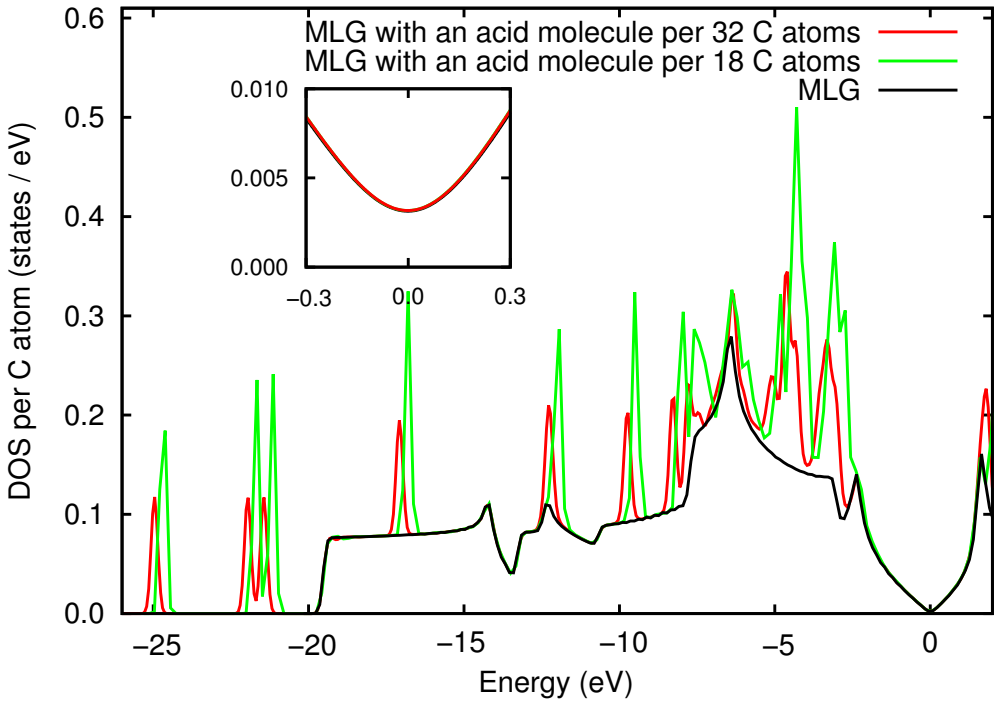

Figure 5. Densities of states per C atom of a monolayer graphene with a chlorosulfonic acid molecule adsorbed per 18 (green line) and 32 carbon atoms (red line). The DOS per C atom of MLG (black line) is given as a reference. The Fermi energy has been used as energy origin.

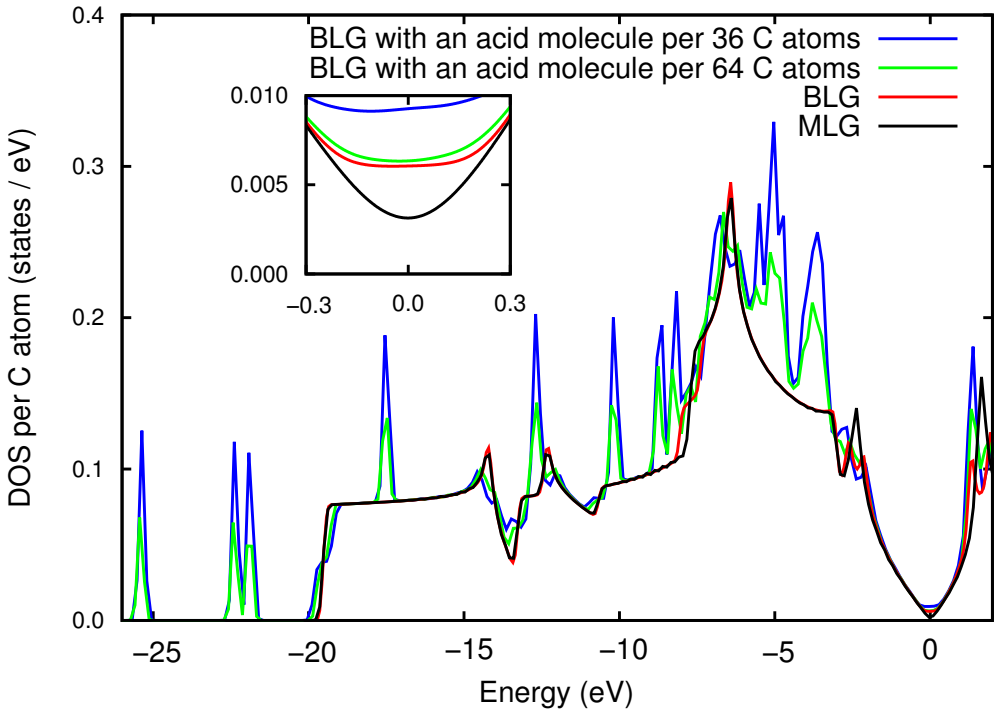

Figure 6. Densities of states per C atom of a bilayer graphene with a chlorosulfonic acid molecule adsorbed per 36 (blue line) and 64 (green line) carbon atoms. The DOS per C atom of MLG (black line) and BLG (red line) is also shown. The Fermi energy has been used as energy origin.

4. Conclusions

We have studied the adsorption of chlorosulfonic acid to MLG and the interaction in between BLG. The adsorption of the acid takes advantage of the good geometric matching of this molecule to the constituent carbon rings, which favors a strong electron depopulation of graphene and, hence, a strong Coulombic repulsion of chlorosulfonic adsorbed graphene layers. Intercalation increases the interlayer distance in BLG and, again, charges positively the layers in an amount that is the highest for several intercalants. This justifies the exfoliating effect of chlorosulfonic acid on graphene. However, at the electronic level, the intercalation of chlorosulfonic acid avoids the complete decoupling of the graphene layers. The charging of the constituent MLG by chlorosulfonic acid is also the basis for understanding the ability of this acid to prevent reaggregation and justifies the high yield of the spontaneous exfoliation and stability of solutions of graphene in chlorosulfonic acid.

Author Contributions: Conceptualization, N.A.C.; methodology, A.B.-A. and N.A.C.; formal analysis, A.B.-A. and N.A.C.; investigation, A.B.-A. and I.G.A.; writing—original draft preparation, A.B.-A.; writing—review and editing, N.A.C.; visualization, A.B.-A. and N.A.C. All authors have read and agreed to the published version of the manuscript.

Funding: This work was supported by the Spanish MICINN and the European Regional Development Fund (grant MAT2014-54378-R) as well as Junta de Castilla y León (grant VA050U14).

Institutional Review Board Statement: Not applicable.

Informed Consent Statement: Not applicable.

Data Availability Statement: The data presented in this study are contained within the article.

Conflicts of Interest: The authors declare no conflict of interest. The funders had no role in the design of the study; in the collection, analyses, or interpretation of data; in the writing of the manuscript; or in the decision to publish the results.

Abbreviations

The following abbreviations are used in this manuscript:

BLG	Bilayer graphene
CSA	Chlorosulfonic acid
CTAB	Cetyltrimethylammonium bromide
DOS	Density of states
DFT	Density Functional Theory
GGA	Generalized Gradient Approximation
HOPG	Highly oriented pyrolytic graphite
LDA	Local Density Approximation
MLG	Monolayer graphene
NPE	Nonylphenolethoxylate
SDBS	Sodium dodecyl benzenesulfonate
SDS	Sodium dodecylsulfate
SNLS	Sodium N-lauroylsarcosinate hydrate

References

1. Novoselov, K.S.; Geim, A.K.; Morozov, S.V.; Jiang, D.; Zhang, Y.; Dubonos, S.V.; Grigorieva, I.V.; Firsov, A.A. Electric Field Effect in Atomically Thin Carbon Films. *Science* **2004**, *306*, 666–669. [CrossRef] [PubMed]
2. Coleman, J.N. Liquid Exfoliation of Defect-Free Graphene. *Accounts Chem. Res.* **2013**, *46*, 14–22. [CrossRef] [PubMed]
3. Blake, P.; Brimicombe, P.D.; Nair, R.R.; Booth, T.J.; Jiang, D.; Schedin, F.; Ponomarenko, L.A.; Morozov, S.V.; Gleeson, H.F.; Hill, E.W.; et al. Graphene-Based Liquid Crystal Device. *Nano Lett.* **2008**, *8*, 1704–1708. [CrossRef] [PubMed]
4. Hernandez, Y.; Nicolosi, V.; Lotya, M.; Blighe, F.M.; Sun, Z.; De, S.; McGovern, I.T.; Holland, B.; Byrne, M.; Gun'ko, Y.K.; et al. High-yield production of graphene by liquid-phase exfoliation of graphite. *Nat. Nanotech.* **2008**, *3*, 563–568. [CrossRef] [PubMed]
5. Khan, U.; O'Neill, A.; Lotya, M.; De, S.; Coleman, J.N. High-Concentration Solvent Exfoliation of Graphene. *Small* **2010**, *6*, 864–871. [CrossRef] [PubMed]
6. Bepete, G.; Anglaret, E.; Ortolani, L.; Morandi, V.; Huang, K.; Pénicaud, A.; Drummond, C. Surfactant-free single-layer graphene in water. *Nat. Chem.* **2017**, *9*, 347–352. [CrossRef]

7. Salavagione, H.J.; Sherwood, J.; De bruyn, M.; Budarin, V.L.; Ellis, G.J.; Clark, J.H.; Shuttleworth, P.S. Identification of high performance solvents for the sustainable processing of graphene. *Green Chem.* **2017**, *19*, 2550–2560. [CrossRef]
8. Nazari, B.; Ranjbar, Z.; Hashjin, R.R.; Rezvani Moghaddam, A.; Momen, G.; Ranjbar, B. Dispersing graphene in aqueous media: Investigating the effect of different surfactants. *Colloids Surfaces A Physicochem. Eng. Asp.* **2019**, *582*, 123870. [CrossRef]
9. Lotya, M.; Hernandez, Y.; King, P.J.; Smith, R.J.; Nicolosi, V.; Karlsson, L.S.; Blighe, F.M.; De, S.; Wang, Z.; McGovern, I.T.; et al. Liquid Phase Production of Graphene by Exfoliation of Graphite in Surfactant/Water Solutions. *J. Am. Chem. Soc.* **2009**, *131*, 3611–3620. [CrossRef]
10. Lotya, M.; King, P.J.; Khan, U.; De, S.; Coleman, J.N. High-Concentration, Surfactant-Stabilized Graphene Dispersions. *ACS Nano* **2010**, *4*, 3155–3162. [CrossRef]
11. Cao, M.; Wang, N.; Wang, L.; Zhang, Y.; Chen, Y.; Xie, Z.; Li, Z.; Pambou, E.; Li, R.; Chen, C.; et al. Direct exfoliation of graphite into graphene in aqueous solutions of amphiphilic peptides. *J. Mater. Chem. B* **2016**, *4*, 152–161. [CrossRef] [PubMed]
12. Englert, J.M.; Röhrl, J.; Schmidt, C.D.; Graupner, R.; Hundhausen, M.; Hauke, F.; Hirsch, A. Soluble Graphene: Generation of Aqueous Graphene Solutions Aided by a Perylenebisimide-Based Bolaamphiphile. *Adv. Mater.* **2009**, *21*, 4265–4269. [CrossRef]
13. Ardyani, T.; Mohamed, A.; Abu Bakar, S.; Sagisaka, M.; Hafiz Mamat, M.; Khairul Ahmad, M.; Ibrahim, S.; Abdul Khalil, H.; King, S.M.; Rogers, S.E.; et al. A guide to designing graphene-philic surfactants. *J. Colloid Interface Sci.* **2022**, *620*, 346–355. [CrossRef] [PubMed]
14. Akter, N.; Mawardi Ayob, M.T.; Radiman, S.; Khandaker, M.U.; Osman, H.; Alamri, S. Bio-Surfactant Assisted Aqueous Exfoliation of High-Quality Few-Layered Graphene. *Crystals* **2021**, *11*, 944. [CrossRef]
15. Sethurajaperumal, A.; Varrla, E. High-Quality and Efficient Liquid-Phase Exfoliation of Few-Layered Graphene by Natural Surfactant. *ACS Sustain. Chem. Eng.* **2022**, *10*, 14746–14760. [CrossRef]
16. Sun, Z.; Huang, X.; Liu, F.; Yang, X.; Rosler, C.; Fischer, R.A.; Muhler, M.; Schuhmann, W. Amine-based solvents for exfoliating graphite to graphene outperform the dispersing capacity of N-methyl-pyrrolidone and surfactants. *Chem. Commun.* **2014**, *50*, 10382–10385. [CrossRef]
17. Gonçalves, R.V.; Maraschin, T.G.; Koppe, G.C.; Dias, L.W.; Balzaretti, N.M.; Galland, G.B.; Regina de Souza Basso, N. Cardanol surfactant/ultrasound-assisted exfoliation of graphite in a water/ethanol solution. *Mater. Chem. Phys.* **2022**, *290*, 126578. [CrossRef]
18. Xiang, Q.; Zhong, B.; Tan, H.; Navik, R.; Liu, Z.; Zhao, Y. Improved Dispersibility of Graphene in an Aqueous Solution by Reduced Graphene Oxide Surfactant: Experimental Verification and Density Functional Theory Calculation. *Langmuir* **2022**, *38*, 8222–8231. [CrossRef]
19. Tambe, P.; Sharma, A.; Kulkarni, H.; Panda, B. Surfactant assisted dispersion of graphene in aqueous solution using mixed surfactants. *Mater. Today Proc.* **2022**, *56*, 1217–1223. [CrossRef]
20. Feng, B.B.; Wang, Z.H.; Suo, W.H.; Wang, Y.; Wen, J.C.; Li, Y.F.; Suo, H.L.; Liu, M.; Ma, L. Performance of graphene dispersion by using mixed surfactants. *Mater. Res. Express* **2020**, *7*, 095009. [CrossRef]
21. Elbourne, A.; McLean, B.; Voïtchovsky, K.; Warr, G.G.; Atkin, R. Molecular Resolution in situ Imaging of Spontaneous Graphene Exfoliation. *J. Phys. Chem. Lett.* **2016**, *7*, 3118–3122. [CrossRef] [PubMed]
22. Tran, T.S.; Dutta, N.K.; Choudhury, N.R. Poly(ionic liquid)-Stabilized Graphene Nanoinks for Scalable 3D Printing of Graphene Aerogels. *ACS Appl. Nano Mater.* **2020**, *3*, 11608–11619. [CrossRef]
23. Bari, R.; Tamas, G.; Irin, F.; Aquino, A.J.; Green, M.J.; Quitevis, E.L. Direct exfoliation of graphene in ionic liquids with aromatic groups. *Colloids Surfaces A Physicochem. Eng. Asp.* **2014**, *463*, 63–69. [CrossRef]
24. You, S.; Sundqvist, B.; Talyzin, A.V. Enormous Lattice Expansion of Hummers Graphite Oxide in Alcohols at Low Temperatures. *ACS Nano* **2013**, *7*, 1395–1399. [CrossRef]
25. Khannanov, A.; Kiiamov, A.; Galyaltdinov, S.; Tayurskii, D.A.; Dimiev, A.M. Pristine graphite oxide retains its C-axis registry in methanol. The way to alternative purification method. *Carbon* **2021**, *173*, 154–162. [CrossRef]
26. Advincula, P.A.; Luong, D.X.; Chen, W.; Raghuraman, S.; Shahsavari, R.; Tour, J.M. Flash graphene from rubber waste. *Carbon* **2021**, *178*, 649–656. [CrossRef]
27. Behabtu, N.; Lomeda, J.R.; Green, M.J.; Higginbotham, A.L.; Sinitskii, A.; Kosynkin, D.V.; Tsentalovich, D.; Parra-Vasquez, A.N.G.; Schmidt, J.; Kesselman, E.; et al. Spontaneous high-concentration dispersions and liquid crystals of graphene. *Nat. Nanotechnol.* **2010**, *5*, 406–411. [CrossRef]
28. Gudarzi, M.M.; Asaad, M.; Mao, B.; Pinter, G.; Guo, J.; Smith, M.; Zhong, X.; Georgiou, T.; Gorbachev, R.; Haigh, S.J.; et al. Chlorosulfuric acid-assisted production of functional 2D materials. *NPJ 2D Mater. Appl.* **2021**, *5*, 35. [CrossRef]
29. Mutlay, I.; Tudoran, L.B. Chlorosulfonic Acid-based Room Temperature Chemical Expansion Route for the Bulk Production of Graphite Nanoplatelets. *Fullerenes Nanotub. Carbon Nanostruct.* **2013**, *21*, 149–157. [CrossRef]
30. Pagona, G.; Bittencourt, C.; Arenal, R.; Tagmatarchis, N. Exfoliated semiconducting pure 2H-MoS2 and 2H-WS2 assisted by chlorosulfonic acid. *Chem. Commun.* **2015**, *51*, 12950–12953. [CrossRef]
31. Du, W.; Jiang, X.; Zhu, L. From graphite to graphene: Direct liquid-phase exfoliation of graphite to produce single- and few-layered pristine graphene. *J. Mater. Chem. A* **2013**, *1*, 10592–10606. [CrossRef]
32. Bernal, J.D. The Structure of Graphite. *Proc. R. Soc. London Ser. A* **1924**, *106*, 749. [CrossRef]
33. Cordero, N.A.; Alonso, J.A. The interaction of sulfuric acid with graphene and formation of adsorbed crystals. *Nanotechnology* **2007**, *18*, 485705. [CrossRef]

34. Ayala, I.G.; Cordero, N.A.; Alonso, J.A. Surfactant effect of sulfuric acid on the exfoliation of bilayer graphene. *Phys. Rev. B* **2011**, *84*, 165424. [CrossRef]
35. Ayala, I.G.; Cordero, N.A. Interaction of sodium bisulfate with mono- and bi-layer graphene. *J. Nanoparticle Res.* **2012**, *14*, 1071. [CrossRef]
36. Ebert, L.B. Intercalation Compounds of Graphite. *Annu. Rev. Mater. Sci.* **1976**, *6*, 181–211. [CrossRef]
37. Samuelson, L.; Batra, I.P. Electronic properties of various stages of lithium intercalated graphite. *J. Phys. C Solid State Phys.* **1980**, *13*, 5105. [CrossRef]
38. Lee, J.K.; Lee, S.C.; Ahn, J.P.; Kim, S.C.; Wilson, J.I.B.; John, P. The growth of AA graphite on (111) diamond. *J. Chem. Phys.* **2008**, *129*, 234709. [CrossRef] [PubMed]
39. Horiuchi, S.; Gotou, T.; Fujiwara, M.; Sotoaka, R.; Hirata, M.; Kimoto, K.; Asaka, T.; Yokosawa, T.; Matsui, Y.; Watanabe, K.; et al. Carbon Nanofilm with a New Structure and Property. *Jpn. J. Appl. Phys.* **2003**, *42*, L1073–L1076. [CrossRef]
40. Liu, Z.; Suenaga, K.; Harris, P.J.F.; Iijima, S. Open and Closed Edges of Graphene Layers. *Phys. Rev. Lett.* **2009**, *102*, 015501. [CrossRef]
41. Kolmogorov, A.N.; Crespi, V.H. Registry-dependent interlayer potential for graphitic systems. *Phys. Rev. B* **2005**, *71*, 235415. [CrossRef]
42. Nanda, B.R.K.; Satpathy, S. Strain and electric field modulation of the electronic structure of bilayer graphene. *Phys. Rev. B* **2009**, *80*, 165430. [CrossRef]
43. Chakarova-Käck, S.D.; Vojvodic, A.; Kleis, J.; Hyldgaard, P.; Schröder, E. Binding of polycyclic aromatic hydrocarbons and graphene dimers in density functional theory. *New J. Phys.* **2010**, *12*, 013017. [CrossRef]
44. Okada, S.; Kobayashi, T. Electronic Properties of Graphite with Rotational Stacking Arrangement. *Jpn. J. Appl. Phys.* **2009**, *48*, 050207. [CrossRef]
45. Hohenberg, P.; Kohn, W. Inhomogeneous Electron Gas. *Phys. Rev.* **1964**, *136*, B864–B871. [CrossRef]
46. Kohn, W.; Sham, L.J. Self-Consistent Equations Including Exchange and Correlation Effects. *Phys. Rev.* **1965**, *140*, A1133–A1138. [CrossRef]
47. Dacapo. Available online: https://wiki.fysik.dtu.dk/dacapo/Introduction (accessed on 26 November 2022).
48. Girifalco, L.A.; Hodak, M. Van der Waals binding energies in graphitic structures. *Phys. Rev. B* **2002**, *65*, 125404. [CrossRef]
49. Hasegawa, M.; Nishidate, K. Semiempirical approach to the energetics of interlayer binding in graphite. *Phys. Rev. B* **2004**, *70*, 205431. [CrossRef]
50. Birowska, M.; Milowska, K.; Majewski, J.A. Van Der Waals Density Functionals for Graphene Layers and Graphite. *Acta Phys. Pol. A* **2011**, *120*, 845–848. [CrossRef]
51. Hod, O. Graphite and hexagonal boron-nitride have the same interlayer distance. Why? *J. Chem. Theory Comput.* **2012**, *8*, 1360–1369. [CrossRef]
52. Torres-Rojas, R.M.; Contreras-Solorio, D.A.; Hernández, L.; Enciso, A. Band gap variation in bi, tri and few-layered 2D graphene/hBN heterostructures. *Solid State Commun.* **2022**, *341*, 114553. [CrossRef]
53. Vanderbilt, D. Soft self-consistent pseudopotentials in a generalized eigenvalue formalism. *Phys. Rev. B* **1990**, *41*, 7892–7895. [CrossRef] [PubMed]
54. Khantha, M.; Cordero, N.A.; Molina, L.M.; Alonso, J.A.; Girifalco, L.A. Interaction of lithium with graphene: An ab initio study. *Phys. Rev. B* **2004**, *70*, 125422. [CrossRef]
55. Khantha, M.; Cordero, N.A.; Alonso, J.A.; Cawkwell, M.; Girifalco, L.A. Interaction and concerted diffusion of lithium in a (5,5) carbon nanotube. *Phys. Rev. B* **2008**, *78*, 115430. [CrossRef]
56. Yokoyama, M.; Nakada, K.; Ishii, A. DFT calculations for SO_4/graphene with and without a Pd atom. *Comput. Mater. Sci.* **2014**, *83*, 418–425. [CrossRef]
57. Monkhorst, H.J.; Pack, J.D. Special points for Brillouin-zone integrations. *Phys. Rev. B* **1976**, *13*, 5188–5192. [CrossRef]
58. Frisch, M.J.; Trucks, G.W.; Schlegel, H.B.; Scuseria, G.E.; Robb, M.A.; Cheeseman, J.R.; Scalmani, G.; Barone, V.; Mennucci, B.; Petersson, G.A.; et al. Gaussian 09. Gaussian Inc. Wallingford CT 2009. Available online: https://gaussian.com/ (accessed on 26 November 2022).
59. Kim, Y.; Hong, S.; Jung, S.; Strano, M.S.; Choi, J.; Baik, S. Dielectrophoresis of surface conductance modulated single-walled carbon nanotubes using catanionic surfactants. *J. Phys. Chem. B* **2006**, *110*, 1541–1545. [CrossRef]
60. Matarredona, O.; Rhoads, H.; Li, Z.R.; Harwell, J.H.; Balzano, L.; Resasco, D.E. Dispersion of single-walled carbon nanotubes in aqueous solutions of the anionic surfactant NaDDBS. *J. Phys. Chem. B* **2003**, *107*, 13357–13367. [CrossRef]
61. Schaefer, D.W.; Brown, J.M.; Anderson, D.P.; Zhao, J.; Chokalingam, K.; Tomlin, D.; Ilavsky, J. Structure and dispersion of carbon nanotubes. *J. Appl. Cryst.* **2003**, *36*, 553–557. [CrossRef]
62. Mulliken, R.S. Electronic Population Analysis on LCAO-MO Molecular Wave Functions. 1. *J. Chem. Phys.* **1955**, *23*, 1833–1840. [CrossRef]
63. Baskin, Y.; Meyer, L. Lattice Constants of Graphite at Low Temperatures. *Phys. Rev.* **1955**, *100*, 544. [CrossRef]
64. Wang, W.; Dai, S.; Li, X.; Yang, J.; Srolovitz, D.J.; Zheng, Q. Measurement of the cleavage energy of graphite. *Nat. Comm.* **2015**, *6*, 8853. [CrossRef] [PubMed]
65. Charlier, J.C.; Gonze, X.; Michenaud, J.P. Graphite Interplanar Bonding: Electronic Delocalization and van der Waals Interaction. *Europhys. Lett.* **1994**, *28*, 403. [CrossRef]

66. Xu, Y.; Li, X.; Dong, J. Infrared and Raman spectra of AA-stacking bilayer graphene. *Nanotechnology* **2010**, *21*, 065711. [CrossRef] [PubMed]
67. Kuganathan, N.; Ganeshalingam, S. Encapsulation and Adsorption of Halogens into Single-Walled Carbon Nanotubes. *Micro* **2021**, *1*, 140–150. [CrossRef]
68. Aoki, M.; Amawashi, H. Dependence of band structures on stacking and field in layered graphene. *Solid State Commun.* **2007**, *142*, 123. [CrossRef]
69. Feng, J.; Qi, L.; Huang, J.Y.; Li, J. Geometric and electronic structure of graphene bilayer edges. *Phys. Rev. B* **2009**, *80*, 165407. [CrossRef]
70. Lee, S.H.; Chiu, C.W.; Lin, M.F. Deformation effects on electronic structures of bilayer graphenes. *Physica E* **2010**, *42*, 732. [CrossRef]
71. Grüneis, A.; Attaccalite, C.; Rubio, A.; Vyalikh, D.V.; Molodtsov, S.L.; Fink, J.; Follath, R.; Eberhardt, W.; Büchner, B.; Pichler, T. Angle-resolved photoemission study of the graphite intercalation compound KC_8: A key to graphene. *Phys. Rev. B* **2009**, *80*, 075431. [CrossRef]